RESEARCH ARTICLE

An interactive meta-analysis of MRI biomarkers of myelin

Matteo Mancini[1,2,3]*, Agah Karakuzu[2], Julien Cohen-Adad[2,4], Mara Cercignani[1,5], Thomas E Nichols[6,7†], Nikola Stikov[2,8†]

[1]Department of Neuroscience, Brighton and Sussex Medical School, University of Sussex, Brighton, United Kingdom; [2]NeuroPoly Lab, Polytechnique Montreal, Montreal, Canada; [3]CUBRIC, Cardiff University, Cardiff, United Kingdom; [4]Functional Neuroimaging Unit, CRIUGM, Université de Montréal, Montreal, Canada; [5]Neuroimaging Laboratory, Fondazione Santa Lucia, Rome, Italy; [6]Wellcome Centre for Integrative Neuroimaging (WIN FMRIB), University of Oxford, Oxford, United Kingdom; [7]Big Data Institute, University of Oxford, Oxford, United Kingdom; [8]Montreal Heart Institute, Université de Montréal, Montreal, Canada

Abstract Several MRI measures have been proposed as in vivo biomarkers of myelin, each with applications ranging from plasticity to pathology. Despite the availability of these myelin-sensitive modalities, specificity and sensitivity have been a matter of discussion. Debate about which MRI measure is the most suitable for quantifying myelin is still ongoing. In this study, we performed a systematic review of published quantitative validation studies to clarify how different these measures are when compared to the underlying histology. We analyzed the results from 43 studies applying meta-analysis tools, controlling for study sample size and using interactive visualization (https://neurolibre.github.io/myelin-meta-analysis). We report the overall estimates and the prediction intervals for the coefficient of determination and find that MT and relaxometry-based measures exhibit the highest correlations with myelin content. We also show which measures are, and which measures are not statistically different regarding their relationship with histology.

***For correspondence:** ingmatteomancini@gmail.com

[†]These authors contributed equally to this work

Competing interests: The authors declare that no competing interests exist.

Funding: See page 13

Received: 28 July 2020
Accepted: 20 October 2020
Published: 21 October 2020

Reviewing editor: Saad Jbabdi, University of Oxford, United Kingdom

Introduction

Myelin is a key component of the central nervous system. The myelin sheaths insulate axons with a triple effect: allowing fast electrical conduction, protecting the axon, and providing trophic support (***Nave and Werner, 2014***). The conduction velocity regulation has become an important research topic, with evidence of activity-dependent myelination as an additional mechanism of plasticity (***Fields, 2015***; ***Sampaio-Baptista and Johansen-Berg, 2017***). Myelin is also relevant from a clinical perspective, given that demyelination is often observed in several neurological diseases such as multiple sclerosis (***Höftberger and Lassmann, 2018***).

Given this important role in pathology and plasticity, measuring myelin in vivo has been an ambitious goal for magnetic resonance imaging (MRI) for more than two decades (***MacKay et al., 1994***; ***Rooney et al., 2007***; ***Stanisz et al., 1999***). Even though the thickness of the myelin sheath is in the order of micrometres, well beyond the MRI spatial resolution, its presence influences several physical properties that can be probed with MRI, from longitudinal and transversal relaxation phenomena to water molecule diffusion processes.

However, being sensitive to myelin is not enough: to study how and why myelin content changes, it is necessary to define a specific biomarker. Interestingly, the quest for measuring myelin has evolved in parallel with an important paradigm shift in MRI research, where MRI data are no longer treated as just 'pictures', but as actual 3D distributions of quantitative measures. This perspective

has breathed new life into an important field of research, quantitative MRI (qMRI), that encompasses the study of how to measure the relevant electromagnetic properties that influence magnetic resonance phenomena in biological tissues (**Cercignani et al., 2018**; **Cohen-Adad and Wheeler-Kingshott, 2014**). From the very definition of qMRI, it is clear that its framework applies to any approach for non-invasive myelin quantification.

Similarly to other qMRI biomarkers, MRI-based myelin measurements are indirect, and might be affected by other microstructural features, making the relationship between these indices and myelination noisy. Assessing the accuracy of such measurements, and their sensitivity to change, is essential for their translation into clinical applications. Validation is therefore a fundamental aspect of their development (**Cohen-Adad, 2018**). The most common approach is based on acquiring MR data from in vivo or ex vivo tissue and then comparing those data with the related samples analyzed using histological techniques. Despite being the most realistic approach, this comparison involves several methodological choices, from the specific technique used as a reference to the quantitative measure used to describe the relationship between MRI and histology. So far, a long list of studies have looked at MRI-histology comparisons (**Cohen-Adad, 2018**; **Laule and Moore, 2018**; **MacKay and Laule, 2016**; **Petiet et al., 2019**), each of them focusing on a specific pathology and a few MRI measures.

Despite these numerous studies, there is still an ongoing debate on what MRI measure should be used to quantify myelin and as a consequence there is a constant methodological effort to propose new measures. This debate would benefit from a quantitative analysis of all the findings published so far, specifically addressing inter-study variations and prospects for future studies, something that is currently missing from the literature.

In this study, we systematically reviewed quantitative MRI-histology comparisons and we used meta-analysis tools to address the following question: how different are the modalities for myelin quantification in terms of their relationship with the underlying histology?

Results

Literature survey

The screening process is summarized in the flowcharts in **Figure 1** and **Appendix 1—figure 1**. The keywords as reported in the appendix returned 688 results on PubMed (last search on 03/06/2020). These results included 50 review articles. From the 50 review articles, six were selected as relevant for both the topics of myelin and related MRI-histology comparisons (**Cohen-Adad, 2018**; **Laule and Moore, 2018**; **Laule et al., 2007**; **MacKay and Laule, 2016**; **Petiet et al., 2019**; **Turner, 2019**). After the assessment, 58 original research studies were considered eligible, as shown in **Appendix 1—table 1** (in the appendix) and Figure S2. All the data collected are available in the supplementary materials (**Source data 1**).

In terms of specific modalities, the survey shows that the most common MRI approach compared with histology was diffusion-weighted imaging (used in 28 studies), followed by magnetization transfer (MT, 27 studies), T2 relaxometry (19 studies) and T1 relaxometry (10 studies). Only 20 studies considered more than one approach: among the others, 20 focused exclusively on diffusion, 12 on MT, and six on T2 relaxometry.

From these 58 studies, we then focused only on brain studies and we further excluded studies not reporting either the number of subjects or the number of ROIs per subject. We also excluded one single-subject study that relied on voxels as distinct samples, whereas the other studies in this review are based on ROIs (i.e. including more than one voxel). In the end, 43 suitable studies were identified for the subsequent analyses.

Meta-analysis

To compare the studies of interest, we first organized them according to the MRI measure used. **Figure 2** and **Figure 3** (and also Figure S3-S4) show the R^2 values for the selected studies across measures: the highest values (R^2 >0.8) are obtained mostly from MT measures, but they are associated with small sample sizes (with an average of 32 sample points). The studies with largest sample sizes are associated with R^2 values between 0.6 and 0.8 for MT and T2 relaxometry, but with lower values for T1 relaxometry and other approaches.

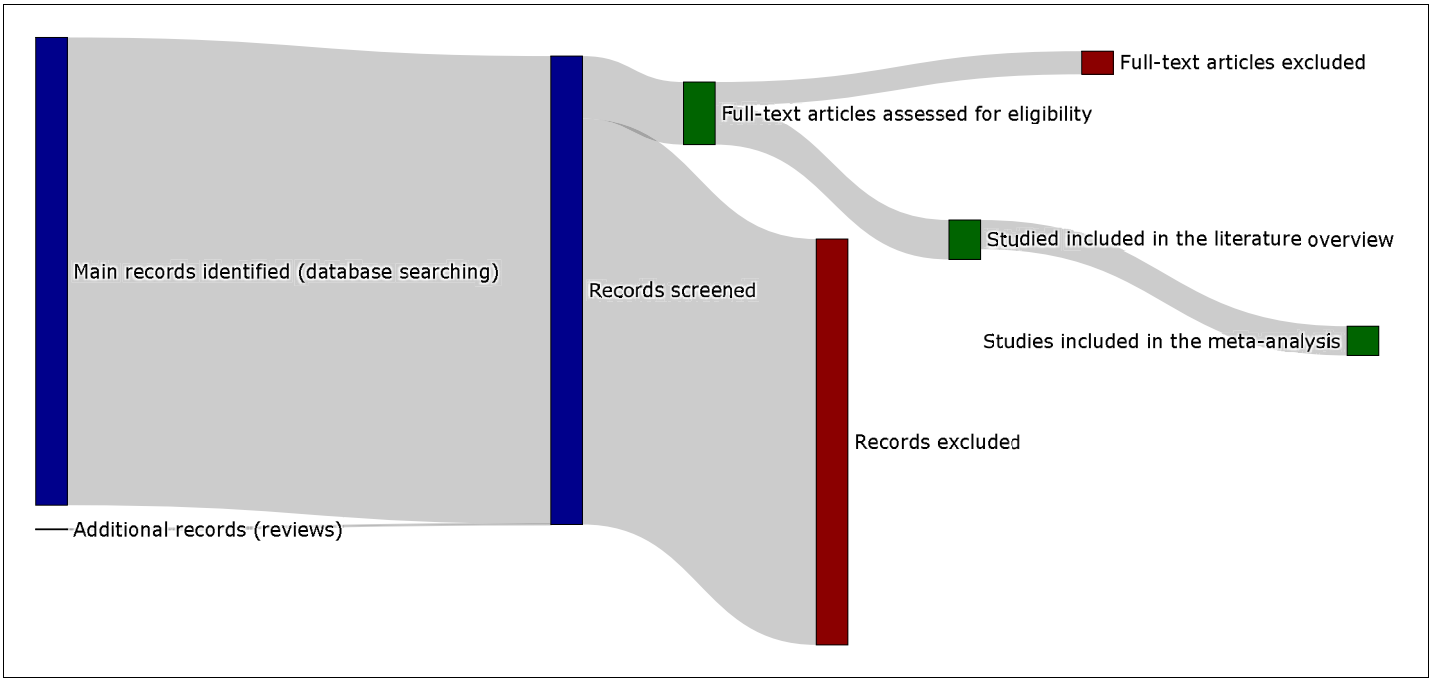

Figure 1. Sankey diagram representing the screening procedure (PRISMA flow chart provided in the appendix). To see the interactive figure: https://neurolibre.github.io/myelin-meta-analysis/01/selection.html#figure-1.

To combine the results for each measure, we then used a mixed-effect model: in this way we were able to express the overall effect size in terms of a range of R^2 values within a confidence interval, but also to assess prediction intervals and inter-study differences. The results are shown as forest plots in ***Figure 4*** (and also Figure S5).

Apart from MPF and MWF, all the measures showed R^2 overall estimates in the range 0.21–0.53. To investigate the significance of the differences between measures, we conducted a repeated measures meta-regression on every R^2 estimate recorded (98 in total over 43 studies). As shown in ***Figure 5*** (and also Figure S6), the measures can be roughly subdivided in two groups: MT- and relaxometry-based measures gave significantly higher R^2 estimates compared to diffusion-based measures. Within the diffusion-based measures, FA shows slightly higher estimates than the others, with marginal significance over RD and AD or no significance in case of MD.

Within MT- and relaxometry-based measures, the trends follow those in the forest plots (***Figure 4***), but most differences are not significant (***Figure 5***). However, the results in terms of z-score give a measure of distance between the R^2 distributions. From this perspective, MPF has higher R^2

Table 1. Results from the mixed-effect models: for each measure we reported the number of studies, the estimate and standard error of the overall R^2 distribution, the τ^2 and the I^2.

Measure	Number of studies	Estimate	Standard error	Tau^2	I^2
MTR	16	0.508	0.0691	0.07	96.03%
MPF	10	0.7657	0.0455	0.0128	83.18%
FA	17	0.3766	0.0663	0.0652	87.49%
RD	15	0.3364	0.0679	0.0615	92.30%
MD	12	0.2639	0.0679	0.044	87.35%
T1	8	0.5321	0.0692	0.0328	86.51%
AD	9	0.2095	0.0802	0.048	97.69%
T2	7	0.3938	0.1023	0.0651	84.49%
MWF	4	0.6997	0.0432	0.0041	73.19%

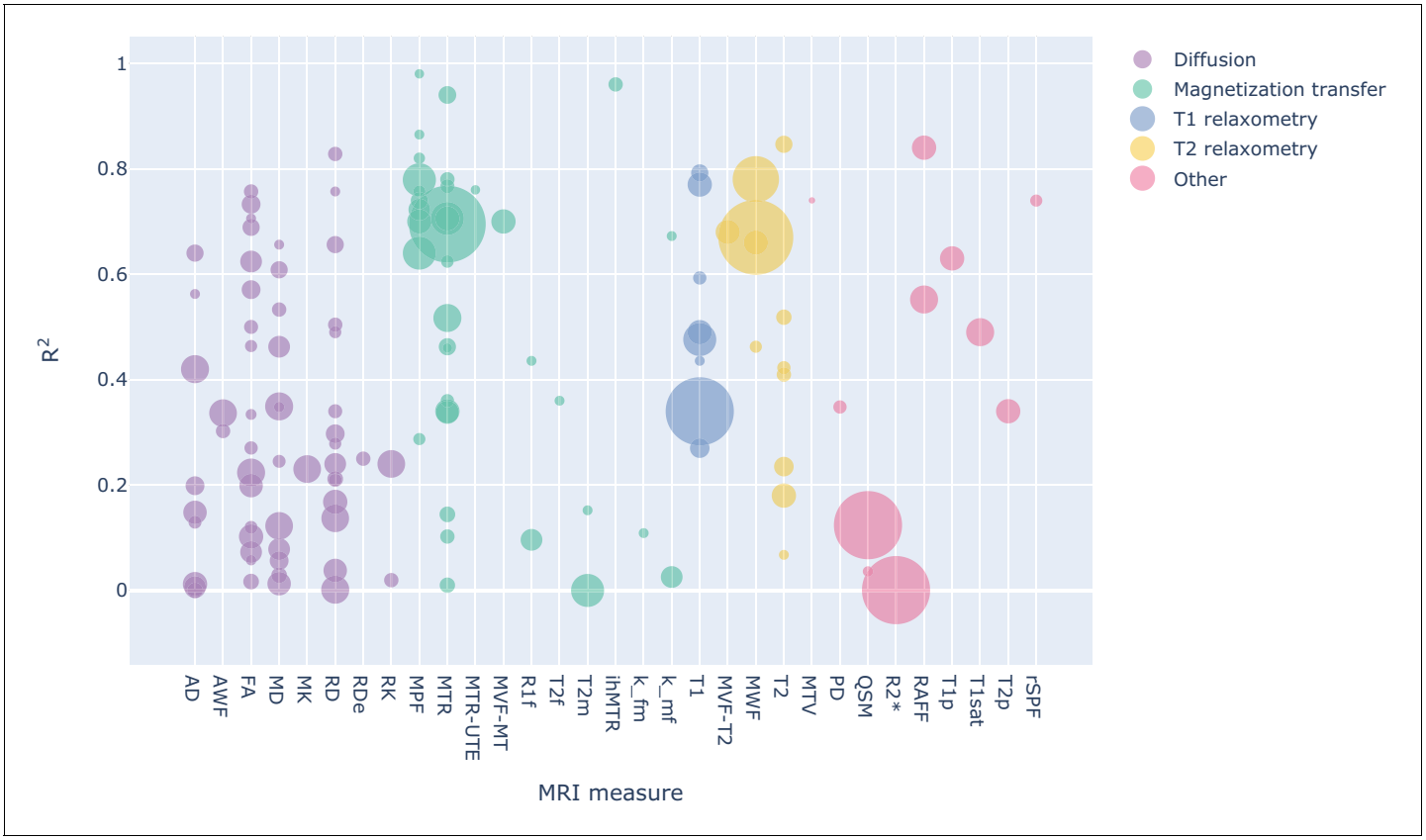

Figure 2. Bubble chart of R^2 values between a given MRI measure and histology for each study across MRI measures, with the area proportional to the number of samples. To see the interactive figure: https://neurolibre.github.io/myelin-meta-analysis/02/closer_look.html#figure-3.

estimates compared to all the other measures, but it is only marginally higher than MWF (z-score = 0.77; p-value=1) so we cannot claim that one is superior to the other. Following the same reasoning, MTR and T1 are not statistically different (z-score = 0.47; p-value=1).

When considering the prediction intervals calculated using τ^2 (the variance of the effect size parameters across the population of studies), for most measures the interval spanned from 0.1 to 0.9 (***Figure 4*** and Figure S5). This implies that future studies relying on such measures can expect, on the basis of these studies, to obtain any R^2 value in this broad interval. The only exceptions were MPF (0.49–1) and MWF (0.45–0.95), whose intervals were narrower than the alternatives. Finally, I^2 (a measure of how much of the variability in a typical study is due to heterogeneity in the experimental design) was generally quite high (***Table 1***). MWF showed the lowest I^2 across measures (I^2 = 73.19%), but this may be misleading considering that it was based on only four studies, while the other measures included around 10 studies. Excluding MWF, MPF also showed a relatively low I^2 (I^2 = 83.18%). Qualitative comparisons across experimental conditions and methodological choices highlighted differences across pathology models, targeted tissue types and reference techniques (***Figure 6*** and Figure S7). Other factors such as magnetic field, co-registration, specific tissue and the related conditions (Figure S8) showed comparable distributions.

Discussion

Indirect measures are the most popular (for better or worse)

The literature survey offers an interesting perspective on popular research trends (Figure S2). The first consideration one can make is that every myelin imaging technique achieves myelin sensitivity through different means. A clear example is offered by the two most common approaches in this meta-analysis, DWI and MT: the MT effect is driven by saturation pulses interacting with myelin

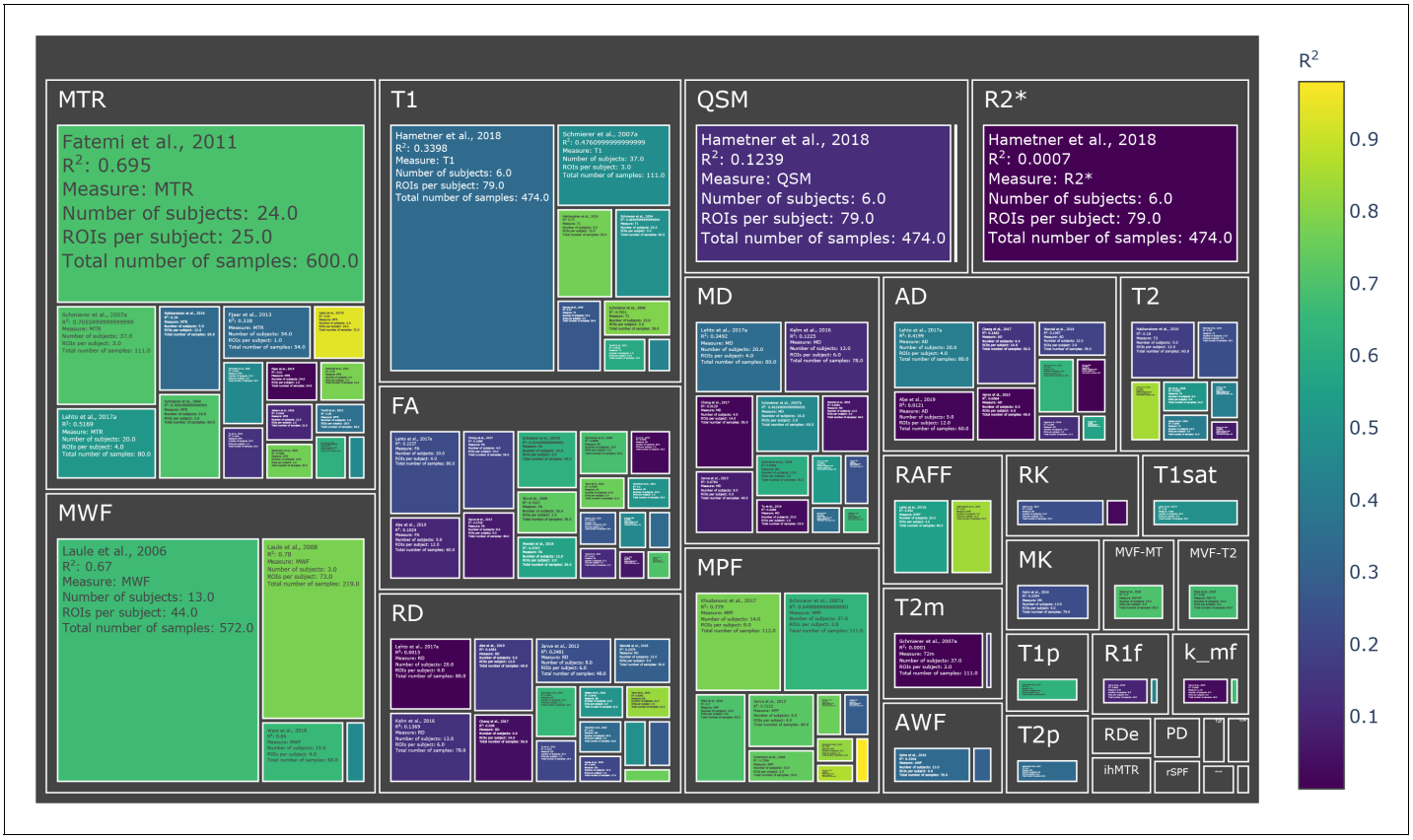

Figure 3. Treemap chart of the studies considered for the meta-analysis, organized by MRI measure. The color of each box represents the reported R^2 value while the size box is proportional to the sample size. To see the interactive figure: https://neurolibre.github.io/myelin-meta-analysis/02/closer_look.html#figure-4.

macromolecules that transfer their magnetization to water, whereas in diffusion experiments myelin is just not part of the picture. Diffusion acquisitions are blind to direct myelin measurement because the TEs used are too long (~100 ms) to be influenced by the actual macromolecules – with T2 of ~ 10 us (***Stanisz et al., 1999***) – or even the water molecules trapped in the myelin sheath – with T2 of ~ 30 ms (***MacKay et al., 1994***). To infer myelin content, one needs to rely on the interaction between intracellular and extracellular water compartments. The majority of diffusion studies included in this analysis used tensor-based measures (with fractional anisotropy being the most common), but some also used kurtosis-based analysis. The main issue with this approach is that other factors affect those measures (***Beaulieu, 2002***; ***Beaulieu, 2009***), making it difficult to specifically relate changes in water compartments to changes in myelin.

Despite this issue, the use of diffusion as a proxy for myelin is quite widespread, specifically outside the field of quantitative MRI. This is probably a consequence of how popular DWI has become and how widely available are the related acquisition sequences. MT, the second most popular technique for quantifying myelin, estimates myelin by acquiring data with and without saturating the macromolecular proton pool. The simplest MT measure, MT ratio (MTR), incorporates non-myelin contributions in the final measurement. Recent acquisition variations include computing MTR from acquisitions with ultra-short echo times (***Du et al., 2009***; ***Guglielmetti et al., 2020***; ***Wei et al., 2018***) or relying on inhomogeneous MT (***Duhamel et al., 2019***; ***Varma et al., 2015***). More complex experiments, for example quantitative MT, are based on fitting two compartments to the data, the free water and the macromolecular compartments, or pools. In this way, one is able to assess myelin through MPF with higher specificity, although still potentially including contributions from other macromolecules. Additional measures have also been considered (including the T2 of each pool, the exchange rate between the pools). The drawback of qMT is the requirement for a longer and more complex acquisition. Recently, there have been alternative techniques to estimate only MPF,

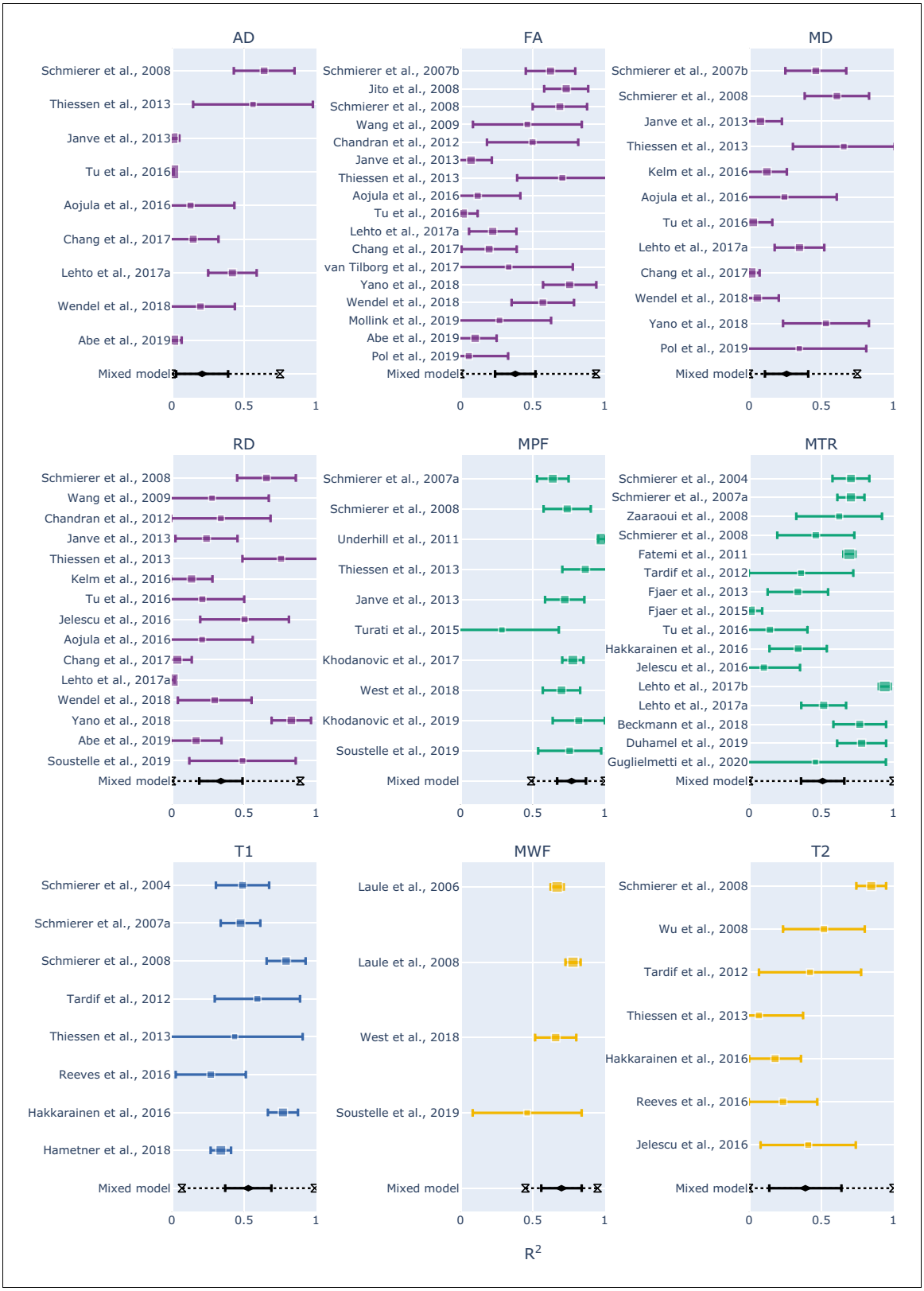

Figure 4. Forest plots showing the R^2 values reported by the studies and estimated from the mixed-effect model for each measure. The hourglasses and the dotted lines in the mixed-effect model outcomes represent the prediction intervals. To see the interactive figure: https://neurolibre.github.io/myelin-meta-analysis/03/meta_analysis.html#figure-5.

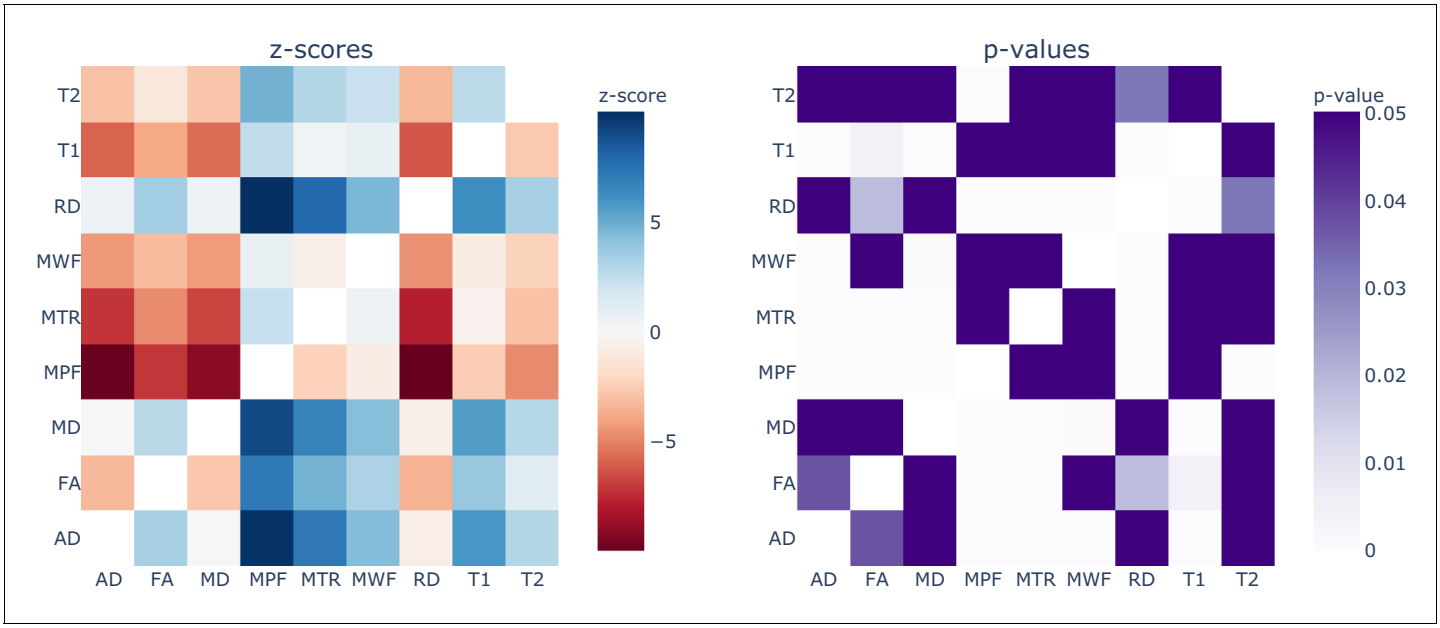

Figure 5. Results from the repeated measures meta-regression, displayed in terms of z-scores (left) and p-values (right) for each pairwise comparison across all the MRI measures. In the z-score heatmap, each element refers to the comparison between the measure on the x axis with the one on the y axis. For example, MPF and FA (z-score = 7.14; p-value<0.0001) are statistically different, while MPF and T1 (z-score = 2.51; p-value=0.43) are not statistically different. To see the interactive figure: https://neurolibre.github.io/myelin-meta-analysis/03/meta_analysis.html#figure-6.

resulting in faster acquisitions with similar results (***Khodanovich et al., 2019***; ***Khodanovich et al., 2017***; ***Yarnykh, 2012***). Despite being focused on macromolecular contributions, these approaches are not strictly specific to myelin (***Sled, 2018***): in this sense, an important limitation is that MT effects are sensitive to the pH of the targeted tissue and therefore changes in the pH (caused for example by inflammation processes) will affect MT-based measures of myelin (***Stanisz et al., 2004***).

Following diffusion and MT, the most popular approach is T2 relaxometry. Unlike diffusion and MT, in T2 relaxometry experiments one can directly observe the contribution from the water trapped between the myelin bilayers, and can therefore estimate the myelin water fraction. A simpler but less specific approach consists in estimating the transverse relaxation time considering the decay to be mono-exponential. A historical and practical drawback of these approaches is that they require longer acquisitions, although faster alternatives have been developed (***Does and Gore, 2000***; ***Prasloski et al., 2012***). A more subtle but nevertheless important limitation lies in the multi-compartment model used in multi-exponential T2 relaxometry (***Does, 2018***): this model generally assumes slow water exchange between compartments, but it has been showed that water exchange actually contributes to T2 spectra variations (***Dula et al., 2010***; ***Harkins et al., 2012***).

Finally, other studies used a diverse collection of other measures, including T1 relaxometry, apparent transversal relaxation rate (R2*), proton density (PD), macromolecular tissue volume (MTV), relaxation along a fictitious field (RAFF), and quantitative susceptibility mapping (QSM).

After this general overview, it is clear that each modality could be a suitable candidate for a quantitative myelin biomarker. To then make a choice informed by the studies here reported, it becomes necessary to consider not only effect sizes in terms of correlation, but also sample sizes and acquisition times.

There is no myelin MRI measure true to histology

When looking at the R^2 values across the different measures, the first detail that catches one's eye is how most measures present a broad range of values (***Figure 2*** and ***Figure 3***). When taking into account the sample size, the largest studies show higher correlations for MT and T2 relaxometry studies than any other approach (Figure S3 and Figure S4). In quantitative terms, the meta-analysis corroborates this idea, showing that MPF and MWF tend to be more specific to myelin compared to the other measures (respectively with R^2 = 0.7657 and R^2 = 0.6997), in line with the underlying

Figure 6. Experimental conditions and methodological choices influencing the R^2 values (top: reference techniques; middle: pathology model; bottom: tissue types). To see the interactive figure: https://neurolibre.github.io/myelin-meta-analysis/04/other_factors.html#figure-7.

theory. Notably, diffusion-based measures show the lowest overall estimates (with values between R^2 = 0.3766 for FA and R^2 = 0.2095 for AD): this could be due to the fact, as already mentioned, that DWI does not specifically measure myelin properties, and despite FA and RD being influenced by the myelin content, they are also influenced by other factors that make them unsuitable as measures of myelin. The repeated measure meta-regression confirms this overall picture, clearly distinguishing MT- and relaxometry-based measures from diffusion-based ones (***Figure 5***).

Despite these considerations on the advantages of MPF and MWF, one should refrain from concluding that they are the 'true' MRI measures of myelin. The reason for this caution is given not by the overall effect sizes observed here, but by the collateral outcomes of the meta-analysis. The first one is given by the prediction intervals: most measures exhibit large intervals (***Figure 4***), not supporting the idea of them being robust biomarkers. MPF and MWF seem to be again the most suitable choices for future studies, but a range between 0.5 and 1 is still quite large.

The second important aspect to consider is given by the differences across studies: the meta-analysis showed how such differences strongly limit inter-study comparisons for a given measure (***Figure 6***). This result should be expected, given that the studies here examined are inevitably influenced by the specific experimental constraints and methodological choices. Given the limited number of studies, it is not possible to quantitatively study interactions between MRI measures and the other factors (e.g. modality used as a reference, tissue types, magnetic field strength). For further qualitative insights, we invite the reader to explore the interactive figures S7-S8. A first important factor to consider is the validation modality used as a reference, which will be dictated by the equipment availability and cost. However, such a choice has an impact on the actual comparison: histology and immunochemistry, despite being specific to myelin, do not offer a volumetric measure of myelin, but rather a proxy based on the transmittance of the histological sections. So far, the only modality able to give a volumetric measure would be electron microscopy, which is an expensive and resource-consuming approach. Also, electron microscopy has several limitations, including tissue shrinkage, degradation of the myelin sheath structure due to imperfect fixation, imperfect penetration of the osmium stain, polishing, keeping focus over large imaging regions. All these effects contribute to the lack of precision and accuracy when quantifying myelin content with EM-based histology (***Cohen-Adad, 2018***). Another important observation is that none of the studies here reviewed considered histology reproducibility, which is hard to quantify as a whole given that a sample can be processed only once: collateral factors affecting tissue processing (e.g. sectioning distortions, mounting and staining issues) constitute an actual limitation for histology-based validation. A further example of influential factor often dictated by equipment availability is the magnetic field strength of the MRI scanner: figure S8 shows that most studies were conducted at 7T and 9.4T, with some pioneering studies at 1.5T and even fewer ones at other field strengths.

In addition to differences in experimental and methodological designs, there are also several considerations that arise out of the lack of shared practices in MRI validation studies. The first evident one is the use of correlations: despite being a simple measure that serves well the purpose of roughly characterizing a relationship, Pearson correlation is not the right tool for quantitative biomarkers, as it does not characterize the actual relationship between histology and MRI. Linear regression is a step forward but has the disadvantage of assuming a linear relationship. Despite Pearson correlation and linear regression being the most common measures used in the studies here reviewed, it is still not clear if the relationship is actually linear. Only one study among the considered ones computed both Pearson and Spearman correlation values (***Tardif et al., 2012***), and reported higher Spearman correlations, pointing out that non-linear relationships should actually be considered. One last consideration regarding the use of correlation measures for validating quantitative biomarkers is about the intercept in the MRI-histology relationship. Notably, only MWF is expected to assume a value equal to zero when myelin is absent (***West et al., 2018***). For the other measures, it would be necessary to estimate the intercept, which leads to the calibration problem in the estimate of myelin volume fraction. Notably, calculating Pearson correlation does not provide any information for such calibration. Another arbitrary practice that would benefit from some harmonization is the choice of ROIs. The studies reported here examined a diverse list of ROIs, in most cases hand-drawn on each modality, encompassing different types of tissue, and the most common approach is to report a single, pooled correlation. This is problematic, as different types of tissue (e.g. grey matter and white matter) will show different values for MRI-based measures but also for histology-based ones, making linearity assumptions about the two modalities. However, with this

approach gross differences between tissues drive the observed correlation, without actually showing if the MRI-based measure under analysis is sensitive to subtle differences and therefore a suitable quantitative biomarker for myelin. The effect of considering different types of tissues is showed in ***Figure 6*** and Figure S7, where correlation ranges change when considering different types of tissue. However, the large correlation range in white matter, the most common tissue studied, suggests that other factors also affect the correlation.

It should be clear at this point that any debate about a universal MRI-based measure of myelin is pointless, at least at the moment, as the overall picture provided by previous studies does not point to any such ideal measure. Nevertheless, is debating about a universal measure helpful for future studies?

Better biomarkers require more reproducibility studies

We hope this meta-analysis convinces the reader that a holy grail of myelin imaging does not exist, at least as long as we consider histology to be the ground truth. Given that we all have to pick our poison, the upside is that measures based on MT and relaxometry are not statistically different, and therefore, future studies have an actual choice among candidate measures. For further progress, rather than debating about a perfect measure, we would argue that what is missing at the moment is a clear picture of what can be achieved with each specific MRI modality. The studies examined here focus on a large set of different measures, and more than half of them considered at most two measures, highlighting how the field is mostly focused on formulating new measures. While it is understood that novel measures can provide new perspectives, it is also fundamentally important to understand the concrete capabilities and limitations of current measures. From this meta-analysis, what the literature clearly lacks is reproducibility studies, specifically answering two main questions: (1) what is the specificity of each measure? We should have a practical validation of our theoretical understanding of the relevant confounds; (2) what is the 'parameter sensitivity' of each measure? Here, we refer to parameter sensitivity in a broad sense, that includes also experimental conditions and methodological choices. The results here presented show how certain conditions (e.g. pathology) seem to affect the coefficient of determination more than others but given the limited number of studies for each modality, we refrained from additional analyses to avoid speculation. A warning message that is evident from these results is the inherent limitation of DWI for estimating myelin content: this is not by any means a novel result (***Beaulieu, 2002***; ***Beaulieu, 2009***), but it is nevertheless worth reiterating given the outcomes of our analysis. If estimating myelin content is relevant in a diffusion study, it is important to consider complementing the diffusion measure with one of the modalities here reviewed; in this way, it would be possible to decouple the influence of myelin content from the many other factors that come into play when considering diffusion phenomena.

Finally, an important factor to take into account when choosing a biomarker of myelin is the actual application. For animal research, long acquisitions are not a major issue. However, when considering biomarkers for potential clinical use, the acquisition time can become a relevant issue. An example is the well-established multi-echo spin-echo implementation of MWF, that can only be used for a specific slice in a hypothetical clinical scenario. Faster techniques have been proposed for estimating it with gradient- and spin-echo (GRASE) sequences (***Does and Gore, 2000***; ***Feinberg and Oshio, 1991***; ***Prasloski et al., 2012***). Even in this case, the acquisition time still reaches 15 min for acquiring roughly the whole brain with an isotropic resolution of 2 mm. Complex MT acquisitions such as qMT suffer from the same problem, although it is possible to use optimized and faster protocols to focus specifically on MPF (***Khodanovich et al., 2019***; ***Khodanovich et al., 2017***; ***Yarnykh, 2012***).

Conclusions

Several MRI measures are sensitive to myelin content and the current literature suggests that most of them are not statistically different in terms of their relationship with the underlying histology. Measures highly correlated with histology are also the ones with a higher expected specificity. This suggests that future studies should try to better address how specific each measure is, for the sake of clarifying suitable applications.

Materials and methods

Review methodology

The Medline database (https://pubmed.ncbi.nlm.nih.gov) was used to retrieve the articles. The keywords used are specified in the appendix. We followed the PRISMA (Preferred Reporting Items for Systematic Reviews and Meta-Analyses) guidelines for record screening and study selection. The results were first screened to remove unrelated work. Specifically we discarded: work relying only on MRI; work relying only on histology or equivalent approaches; work reporting only qualitative comparisons. After this first screening, the remaining papers were assessed. At this stage, we discarded: studies using MRI-based measures in arbitrary units (e.g. T1-weighted or T2-weighted data); studies using measures of variation in myelin content (defined either as the difference between normal and abnormal myelin content) either for MRI or for histology; studies using arbitrary assessment scales; studies comparing MRI-based absolute measures of myelin with histology-based relative measures (e.g. g-ratio); studies reporting other quantitative measures than correlation or R^2 values; studies comparing histology from one dataset and MRI from a different one. As an additional source for potential candidate studies, we screened the review articles in the initial results, and we selected the relevant studies that were not already present in the studies already selected.

From the final papers, we collected first the following details: the DOI; which approach was used (diffusion, MT, T1 relaxometry, T2 relaxometry, or other); which specific MRI measures were compared to histology or equivalent techniques; the magnetic field; the technique used as a reference (histology, immunochemistry, microscopy, electron microscopy); the focus of the study in terms of brain, spinal cord or peripheral nerve; if the subjects were humans or animals, and if the latter which animal; if the tissue under exam was in vivo, in situ or ex vivo, and in the latter case if the tissue was fixed or not; if the tissue was healthy or pathological, and if the latter which pathology; the specific structures examined for correlation purposes; which comparison technique was used (e.g. Pearson correlation, Spearman correlation, linear regression); the number of subjects; the number of ROIs per subject; the male/female ratio; if registration procedures were performed to align MRI and histology; in case of pathological tissue, if control tissue was considered as well; other relevant notes. If before calculating the correlations the data were averaged across subjects, the number of subjects was considered to be one. The same consideration was made for averaging across ROIs. This is because the numbers of subjects and ROIs were used to take into account how many sample points were used when computing the correlation. We set each of those numbers to one for all the studies where the data were averaged respectively across subjects and across ROIs. Finally, in those cases where the number of ROIs or the number of subjects were given as a range rather than specific values, we used the most conservative value and added the related details to the notes.

We then proceeded to collect the quantitative results reported for each measure and for each study in the form of R^2. Given that different studies may rely on a different strategy when reporting correlations, we adopted the following reasoning to limit discrepancies across studies while still objectively representing each of them. In case of multiple correlation values reported, for our analysis we selected the ones referring to the whole dataset and the entire brain if available, and considering each ROI in a given subject as a sample if possible; if only correlation values for specific ROIs were reported, the one for the most common reported structure would be chosen. In the case of multiple subjects, if data were provided separately for each group, the correlation for the control group was used. When different comparison methods were reported (e.g. both Pearson and Spearman correlation) or if the MRI data was compared with multiple references (e.g. both histology and immunohistochemistry), the correlations used were chosen on the basis of the following priority orders (from the most preferable to the least): for multiple comparison methods, linear regression, Spearman correlation, Pearson correlation; for multiple reference techniques, electron microscopy, immunohistochemistry, histology. Finally, in any other case where more than one correlation value was available, the most conservative value was used. Any other additional value was in any case mentioned in the notes of the respective study.

Meta-analysis

For the quantitative analysis, we restricted our focus on brain studies and only on the ones providing an indication of both the number of subjects and the number of ROIs. For each study, we computed

the sample size as the product between the number of subjects and the number of ROIs per subject. In this way, we were able to compare the reported R^2 values across measures taking into account the related number of points actually used for correlation purposes. We note that correlation or regression analyses run on multiple ROIs and subjects represents a repeated measures analysis, for which the degrees of freedom computation can be complex; however, most papers neglected the repeated measures structure of the data and thus the sample size computation here represents a very approximate and optimistic view of the precision of each R^2 value.

To estimate the variance of each R^2 value, we relied on the correlation properties and the delta method (***Lehman, 1999***). Let us consider the Pearson's correlation r of two variables X and Y with population correlation ρ. If r is calculated from N random samples, the sampling variance is $(1-\rho^2)^2/N$. Applying the delta method, we then approximated the variance of R^2 as $4\ R^2(1\ R^2)^2/N$, assuming $R^2 \approx \rho^2$. As we recognise that some papers computed Spearman correlation, this calculation is again optimistic and may underestimate the sampling variability of the squared Spearman correlation.

To estimate the overall effect size in terms of R^2, we have to choose how to model the distribution of true effects given by the data collected from the literature. The two most common approaches are fixed-effects and mixed-effects models. While the underlying mathematical model is the same as the one used for linear regression (more details in the appendix), the assumptions are different: fixed-effects models assume that all the studies share a common effect size, while mixed-effects models assume that the effect size across studies is similar but not identical (***Raudenbush, 2009***). In our case, as the studies have several factors that influence the R^2 values (e.g. histology/microscopy reference, magnetic field strength, pathology model), we expect a distribution of effect sizes due to inter-study differences. This is why we proceeded to fit a mixed-effects model to each measure that was featured in more than two studies. Apart from the effect size distributions, we reported two additional measures, I^2 and τ^2: the former expresses as a percentage how much of variability in a typical study is due to heterogeneity (i.e. the variation in study outcomes between studies) rather than chance (***Higgins and Thompson, 2002***), while the latter can be used to calculate the prediction interval (***Raudenbush, 2009***), which gives the expected range for the measure of interest in future studies. We used forest plots to represent the outcomes, and both the mixed effects estimate of the population estimated R^2, with both a 95% confidence and a (larger) 95% prediction interval.

For the explicit purpose of comparing the effect sizes between different MRI measures, we conducted a repeated measures meta-regression on every R^2 value recorded. We associated each R^2 value with three additional details: (i) the related variance, as done in the measure-specific mixed-effects models; (ii) the related study, used as the random intercept (i.e. random variable) to incorporate potential inter-study variability; and (iii) the related MRI measure, used as the moderator (i.e. categorical variable) to estimate the differences between measures. In this way, the meta-regression leads to R^2 intervals for each MRI measure, with the same trend as measure-specific mixed-effects models but with subtle differences. This is because the meta-regression makes two additional assumptions: first, R^2 estimates within the same study share the same random effects and second, the between-study variance is the same for all observations. We then used the meta-regression R^2 estimates to compute every possible pairwise comparison between MRI measures and to identify significantly different pairs using Tukey's test, while controlling the error rate over all the possible comparisons (Bonferroni correction).

This additional model is necessary, as direct comparisons are not possible with measure-specific analyses. While the repeated measures meta-regression makes direct comparisons straightforward, we reported the main R^2 estimates based on the measure-specific mixed-effects models, as they make weaker assumptions.

For visual comparisons, we used the Jupyter notebook provided in the supplementary materials. For model fitting, we used the Metafor package, version 2.4–0 (***Viechtbauer, 2010***).

Acknowledgements

MM was funded by the Wellcome Trust through a Sir Henry Wellcome Postdoctoral Fellowship [213722/Z/18/Z]. TEN was supported by NIH grant R01MH096906.

Additional information

Funding

Funder	Grant reference number	Author
Wellcome Trust	213722/Z/18/Z	Matteo Mancini
National Institutes of Health	R01MH096906	Thomas E Nichols

The funders had no role in study design, data collection and interpretation, or the decision to submit the work for publication.

Author contributions

Matteo Mancini, Conceptualization, Data curation, Formal analysis, Visualization, Methodology, Writing - original draft, Writing - review and editing; Agah Karakuzu, Visualization, Writing - review and editing; Julien Cohen-Adad, Mara Cercignani, Conceptualization, Writing - review and editing; Thomas E Nichols, Nikola Stikov, Conceptualization, Methodology, Writing - review and editing

Author ORCIDs

Matteo Mancini https://orcid.org/0000-0001-7194-4568
Agah Karakuzu https://orcid.org/0000-0001-7283-271X
Julien Cohen-Adad https://orcid.org/0000-0003-3662-9532
Mara Cercignani https://orcid.org/0000-0002-4550-2456
Thomas E Nichols https://orcid.org/0000-0002-4516-5103
Nikola Stikov http://orcid.org/0000-0002-8480-5230

Decision letter and Author response

Decision letter https://doi.org/10.7554/eLife.61523.sa1
Author response https://doi.org/10.7554/eLife.61523.sa2

Additional files

Supplementary files

- Source code 1. A Jupyter notebook in ipynb format containing the Python code used to process the data, run the analyses and generate all the figures. In order to execute the notebook, the Python (3.7) and R (3.6) interpreters are required, as well as the R packages metafor (2.4) and multcomp (1.4), and the following Python packages: numpy (1.18.4); pandas (0.25.3); plotly (4.8.1); rpy2 (3.3.4); xlrd (1.2.0). The notebook assumes that the spreadsheet is in the same path as the notebook itself. More details are provided here: https://github.com/matteomancini/myelin-meta-analysis (***Mancini, 2020***; copy archived at swh:1:rev:17ca8673c9e15c54ad0b814248b69232b63c3a38).
- Source data 1. A spreadsheet in xlsx format containing all the data and details collected for the studies considered in this systematic review.
- Supplementary file 1. A multimedia file in HTML format containing an interactive version of the figures in this manuscript plus additional ones.
- Transparent reporting form

Data availability

All the data collected from the selected studies for this meta-analysis are provided in the spreadsheet file Source data 1.

References

Abe Y, Komaki Y, Seki F, Shibata S, Okano H, Tanaka KF. 2019. Correlative study using structural MRI and super-resolution microscopy to detect structural alterations induced by long-term optogenetic stimulation of striatal medium spiny neurons. *Neurochemistry International* **125**:163–174. DOI: https://doi.org/10.1016/j.neuint.2019.02.017, PMID: 30825601

Aojula A, Botfield H, McAllister JP, Gonzalez AM, Abdullah O, Logan A, Sinclair A. 2016. Diffusion tensor imaging with direct cytopathological validation: characterisation of decorin treatment in experimental juvenile communicating hydrocephalus. *Fluids and Barriers of the CNS* **13**:9. DOI: https://doi.org/10.1186/s12987-016-0033-2

Beaulieu C. 2002. The basis of anisotropic water diffusion in the nervous system - a technical review. *NMR in Biomedicine* **15**:435–455. DOI: https://doi.org/10.1002/nbm.782, PMID: 12489094

Beaulieu C. 2009. CHAPTER 6 - The Biological Basis of Diffusion Anisotropy. In: Johansen-Berg H, Behrens T. E. J (Eds). *Diffusion MRI*. Academic Press. p. 105–126.

Beckmann N, Giorgetti E, Neuhaus A, Zurbruegg S, Accart N, Smith P, Perdoux J, Perrot L, Nash M, Desrayaud S, Wipfli P, Frieauff W, Shimshek DR. 2018. Brain region-specific enhancement of remyelination and prevention of demyelination by the CSF1R kinase inhibitor BLZ945. *Acta Neuropathologica Communications* **6**:9. DOI: https://doi.org/10.1186/s40478-018-0510-8, PMID: 29448957

Berman S, West KL, Does MD, Yeatman JD, Mezer AA. 2018. Evaluating g-ratio weighted changes in the corpus callosum as a function of age and sex. *NeuroImage* **182**:304–313. DOI: https://doi.org/10.1016/j.neuroimage.2017.06.076, PMID: 28673882

Cercignani M, Dowell NG, Tofts PS. 2018. *Quantitative MRI of the Brain*. CRC Press.

Chandran P, Upadhyay J, Markosyan S, Lisowski A, Buck W, Chin CL, Fox G, Luo F, Day M. 2012. Magnetic resonance imaging and histological evidence for the blockade of cuprizone-induced demyelination in C57BL/6 mice. *Neuroscience* **202**:446–453. DOI: https://doi.org/10.1016/j.neuroscience.2011.10.051, PMID: 22119061

Chang EH, Argyelan M, Aggarwal M, Chandon TS, Karlsgodt KH, Mori S, Malhotra AK. 2017. Diffusion tensor imaging measures of white matter compared to myelin basic protein immunofluorescence in tissue cleared intact brains. *Data in Brief* **10**:438–443. DOI: https://doi.org/10.1016/j.dib.2016.12.018, PMID: 28054004

Chen HS, Holmes N, Liu J, Tetzlaff W, Kozlowski P. 2017. Validating myelin water imaging with transmission electron microscopy in a rat spinal cord injury model. *NeuroImage* **153**:122–130. DOI: https://doi.org/10.1016/j.neuroimage.2017.03.065, PMID: 28377211

Cohen-Adad J. 2018. Microstructural imaging in the spinal cord and validation strategies. *NeuroImage* **182**:169–183. DOI: https://doi.org/10.1016/j.neuroimage.2018.04.009, PMID: 29635029

Cohen-Adad J, Wheeler-Kingshott CA. 2014. *Quantitative MRI of the Spinal Cord*. Academic Press.

Does MD. 2018. Inferring brain tissue composition and microstructure via MR relaxometry. *NeuroImage* **182**:136–148. DOI: https://doi.org/10.1016/j.neuroimage.2017.12.087, PMID: 29305163

Does MD, Gore JC. 2000. Rapid acquisition transverse relaxometric imaging. *Journal of Magnetic Resonance* **147**:116–120. DOI: https://doi.org/10.1006/jmre.2000.2168, PMID: 11042054

Du J, Takahashi AM, Bydder M, Chung CB, Bydder GM. 2009. Ultrashort TE imaging with off-resonance saturation contrast (UTE-OSC). *Magnetic Resonance in Medicine* **62**:527–531. DOI: https://doi.org/10.1002/mrm.22007, PMID: 19449436

Duhamel G, Prevost VH, Cayre M, Hertanu A, Mchinda S, Carvalho VN, Varma G, Durbec P, Alsop DC, Girard OM. 2019. Validating the sensitivity of inhomogeneous magnetization transfer (ihMT) MRI to myelin with fluorescence microscopy. *NeuroImage* **199**:289–303. DOI: https://doi.org/10.1016/j.neuroimage.2019.05.061, PMID: 31141736

Dula AN, Gochberg DF, Valentine HL, Valentine WM, Does MD. 2010. Multiexponential *T2,* magnetization transfer, and quantitative histology in white matter tracts of rat spinal cord. *Magnetic Resonance in Medicine* **63**:902–909. DOI: https://doi.org/10.1002/mrm.22267, PMID: 20373391

Fatemi A, Wilson MA, Phillips AW, McMahon MT, Zhang J, Smith SA, Arauz EJ, Falahati S, Gummadavelli A, Bodagala H, Mori S, Johnston MV. 2011. *In vivo* magnetization transfer MRI shows dysmyelination in an ischemic mouse model of periventricular leukomalacia. *Journal of Cerebral Blood Flow & Metabolism* **31**:2009–2018. DOI: https://doi.org/10.1038/jcbfm.2011.68, PMID: 21540870

Feinberg DA, Oshio K. 1991. GRASE (gradient- and spin-echo) MR imaging: a new fast clinical imaging technique. *Radiology* **181**:597–602. DOI: https://doi.org/10.1148/radiology.181.2.1924811, PMID: 1924811

Fields RD. 2015. A new mechanism of nervous system plasticity: activity-dependent myelination. *Nature Reviews Neuroscience* **16**:756–767. DOI: https://doi.org/10.1038/nrn4023, PMID: 26585800

Fjær S, Bo L, Lundervold A, Myhr KM, Pavlin T, Torkildsen O, Wergeland S. 2013. Deep gray matter demyelination detected by magnetization transfer ratio in the cuprizone model. *PLOS ONE* **8**:e84162. DOI: https://doi.org/10.1371/journal.pone.0084162, PMID: 24386344

Fjær S, Bo L, Myhr KM, Torkildsen Ø, Wergeland S. 2015. Magnetization transfer ratio does not correlate to myelin content in the brain in the MOG-EAE mouse model. *Neurochemistry International* **83-84**:28–40. DOI: https://doi.org/10.1016/j.neuint.2015.02.006, PMID: 25744931

Guglielmetti C, Boucneau T, Cao P, Van der Linden A, Larson PEZ, Chaumeil MM. 2020. Longitudinal evaluation of demyelinated lesions in a multiple sclerosis model using ultrashort Echo time magnetization transfer (UTE-MT) imaging. *NeuroImage* **208**:116415. DOI: https://doi.org/10.1016/j.neuroimage.2019.116415, PMID: 31811900

Hakkarainen H, Sierra A, Mangia S, Garwood M, Michaeli S, Gröhn O, Liimatainen T. 2016. MRI relaxation in the presence of fictitious fields correlates with myelin content in normal rat brain. *Magnetic Resonance in Medicine* **75**:161–168. DOI: https://doi.org/10.1002/mrm.25590

Hametner S, Endmayr V, Deistung A, Palmrich P, Prihoda M, Haimburger E, Menard C, Feng X, Haider T, Leisser M, Köck U, Kaider A, Höftberger R, Robinson S, Reichenbach JR, Lassmann H, Traxler H, Trattnig S, Grabner G. 2018. The influence of brain iron and myelin on magnetic susceptibility and effective transverse relaxation - A biochemical and histological validation study. *NeuroImage* **179**:117–133. DOI: https://doi.org/10.1016/j.neuroimage.2018.06.007, PMID: 29890327

Harkins KD, Dula AN, Does MD. 2012. Effect of intercompartmental water exchange on the apparent myelin water fraction in multiexponential *T2* measurements of rat spinal cord. *Magnetic Resonance in Medicine* **67**:793–800. DOI: https://doi.org/10.1002/mrm.23053, PMID: 21713984

Harkins KD, Valentine WM, Gochberg DF, Does MD. 2013. In-vivo multi-exponential T2, magnetization transfer and quantitative histology in a rat model of intramyelinic edema. *NeuroImage: Clinical* **2**:810–817. DOI: https://doi.org/10.1016/j.nicl.2013.06.007

Higgins JP, Thompson SG. 2002. Quantifying heterogeneity in a meta-analysis. *Statistics in Medicine* **21**:1539–1558. DOI: https://doi.org/10.1002/sim.1186, PMID: 12111919

Höftberger R, Lassmann H. 2018. Chapter 19 - Inflammatory demyelinating diseases of the central nervous system. In: Kovacs G. G, Alafuzoff I (Eds). *Handbook of Clinical Neurology*. Elsevier. p. 263–283.

Janve VA, Zu Z, Yao SY, Li K, Zhang FL, Wilson KJ, Ou X, Does MD, Subramaniam S, Gochberg DF. 2013. The radial diffusivity and magnetization transfer pool size ratio are sensitive markers for demyelination in a rat model of type III multiple sclerosis (MS) lesions. *NeuroImage* **74**:298–305. DOI: https://doi.org/10.1016/j.neuroimage.2013.02.034, PMID: 23481461

Jelescu IO, Zurek M, Winters KV, Veraart J, Rajaratnam A, Kim NS, Babb JS, Shepherd TM, Novikov DS, Kim SG, Fieremans E. 2016. In vivo quantification of demyelination and recovery using compartment-specific diffusion MRI metrics validated by electron microscopy. *NeuroImage* **132**:104–114. DOI: https://doi.org/10.1016/j.neuroimage.2016.02.004, PMID: 26876473

Jito J, Nakasu S, Ito R, Fukami T, Morikawa S, Inubushi T. 2008. Maturational changes in diffusion anisotropy in the rat corpus callosum: comparison with quantitative histological evaluation. *Journal of Magnetic Resonance Imaging* **28**:847–854. DOI: https://doi.org/10.1002/jmri.21496, PMID: 18821626

Kelm ND, West KL, Carson RP, Gochberg DF, Ess KC, Does MD. 2016. Evaluation of diffusion kurtosis imaging in ex vivo hypomyelinated mouse brains. *NeuroImage* **124**:612–626. DOI: https://doi.org/10.1016/j.neuroimage.2015.09.028, PMID: 26400013

Khodanovich MY, Sorokina IV, Glazacheva VY, Akulov AE, Nemirovich-Danchenko NM, Romashchenko AV, Tolstikova TG, Mustafina LR, Yarnykh VL. 2017. Histological validation of fast macromolecular proton fraction mapping as a quantitative myelin imaging method in the cuprizone demyelination model. *Scientific Reports* **7**:46686. DOI: https://doi.org/10.1038/srep46686, PMID: 28436460

Khodanovich M, Pishchelko A, Glazacheva V, Pan E, Akulov A, Svetlik M, Tyumentseva Y, Anan'ina T, Yarnykh V. 2019. Quantitative imaging of white and gray matter remyelination in the cuprizone demyelination model using the macromolecular proton fraction. *Cells* **8**:1204. DOI: https://doi.org/10.3390/cells8101204

Kozlowski P, Raj D, Liu J, Lam C, Yung AC, Tetzlaff W. 2008. Characterizing white matter damage in rat spinal cord with quantitative MRI and histology. *Journal of Neurotrauma* **25**:653–676. DOI: https://doi.org/10.1089/neu.2007.0462, PMID: 18578635

Kozlowski P, Rosicka P, Liu J, Yung AC, Tetzlaff W. 2014. In vivo longitudinal myelin water imaging in rat spinal cord following dorsal column transection injury. *Magnetic Resonance Imaging* **32**:250–258. DOI: https://doi.org/10.1016/j.mri.2013.12.006, PMID: 24462106

Laule C, Leung E, Lis DK, Traboulsee AL, Paty DW, MacKay AL, Moore GR. 2006. Myelin water imaging in multiple sclerosis: quantitative correlations with histopathology. *Multiple Sclerosis Journal* **12**:747–753. DOI: https://doi.org/10.1177/1352458506070928, PMID: 17263002

Laule C, Vavasour IM, Kolind SH, Li DK, Traboulsee TL, Moore GR, MacKay AL. 2007. Magnetic resonance imaging of myelin. *Neurotherapeutics* **4**:460–484. DOI: https://doi.org/10.1016/j.nurt.2007.05.004, PMID: 17599712

Laule C, Kozlowski P, Leung E, Li DK, Mackay AL, Moore GR. 2008. Myelin water imaging of multiple sclerosis at 7 T: correlations with histopathology. *NeuroImage* **40**:1575–1580. DOI: https://doi.org/10.1016/j.neuroimage.2007.12.008, PMID: 18321730

Laule C, Vavasour IM, Leung E, Li DK, Kozlowski P, Traboulsee AL, Oger J, Mackay AL, Moore GR. 2011. Pathological basis of diffusely abnormal white matter: insights from magnetic resonance imaging and histology. *Multiple Sclerosis Journal* **17**:144–150. DOI: https://doi.org/10.1177/1352458510384008, PMID: 20965961

Laule C, Moore GRW. 2018. Myelin water imaging to detect demyelination and remyelination and its validation in pathology. *Brain Pathology* **28**:750–764. DOI: https://doi.org/10.1111/bpa.12645, PMID: 30375119

Lehman EL. 1999. *Elements of Large-Sample Theory*. Springer.

Lehto LJ, Albors AA, Sierra A, Tolppanen L, Eberly LE, Mangia S, Nurmi A, Michaeli S, Gröhn O. 2017a. Lysophosphatidyl choline induced demyelination in rat probed by relaxation along a fictitious field in high rank rotating frame. *Frontiers in Neuroscience* **11**:433. DOI: https://doi.org/10.3389/fnins.2017.00433, PMID: 28824359

Lehto LJ, Sierra A, Gröhn O. 2017b. Magnetization transfer SWIFT MRI consistently detects histologically verified myelin loss in the thalamocortical pathway after a traumatic brain injury in rat. *NMR in Biomedicine* **30**::e3678. DOI: https://doi.org/10.1002/nbm.3678

MacKay A, Whittall K, Adler J, Li D, Paty D, Graeb D. 1994. In vivo visualization of myelin water in brain by magnetic resonance. *Magnetic Resonance in Medicine* **31**:673–677. DOI: https://doi.org/10.1002/mrm.1910310614, PMID: 8057820

MacKay AL, Laule C. 2016. Magnetic resonance of myelin water: an in vivo Marker for Myelin. *Brain Plasticity* **2**: 71–91. DOI: https://doi.org/10.3233/BPL-160033

Mancini M. 2020. myelin-meta-analysis. *GitHub*. 17ca867. https://github.com/matteomancini/myelin-meta-analysis

Mollink J, Hiemstra M, Miller KL, Huszar IN, Jenkinson M, Raaphorst J, Wiesmann M, Ansorge O, Pallebage-Gamarallage M, van Cappellen van Walsum AM. 2019. White matter changes in the perforant path area in patients with amyotrophic lateral sclerosis. *Neuropathology and Applied Neurobiology* **45**:570–585. DOI: https://doi.org/10.1111/nan.12555, PMID: 31002412

Nave KA, Werner HB. 2014. Myelination of the nervous system: mechanisms and functions. *Annual Review of Cell and Developmental Biology* **30**:503–533. DOI: https://doi.org/10.1146/annurev-cellbio-100913-013101, PMID: 25288117

Odrobina EE, Lam TY, Pun T, Midha R, Stanisz GJ. 2005. MR properties of excised neural tissue following experimentally induced demyelination. *NMR in Biomedicine* **18**:277–284. DOI: https://doi.org/10.1002/nbm.951, PMID: 15948233

Peters JM, Struyven RR, Prohl AK, Vasung L, Stajduhar A, Taquet M, Bushman JJ, Lidov H, Singh JM, Scherrer B, Madsen JR, Prabhu SP, Sahin M, Afacan O, Warfield SK. 2019. White matter mean diffusivity correlates with myelination in tuberous sclerosis complex. *Annals of Clinical and Translational Neurology* **6**:1178–1190. DOI: https://doi.org/10.1002/acn3.793, PMID: 31353853

Petiet A, Adanyeguh I, Aigrot MS, Poirion E, Nait-Oumesmar B, Santin M, Stankoff B. 2019. Ultrahigh field imaging of myelin disease models: toward specific markers of myelin integrity? *Journal of Comparative Neurology* **527**:2179–2189. DOI: https://doi.org/10.1002/cne.24598, PMID: 30520034

Pol S, Sveinsson M, Sudyn M, Babek N, Siebert D, Bertolino N, Modica CM, Preda M, Schweser F, Zivadinov R. 2019. Teriflunomide's Effect on Glia in Experimental Demyelinating Disease: A Neuroimaging and Histologic Study. *Journal of Neuroimaging* **29**:52–61. DOI: https://doi.org/10.1111/jon.12561, PMID: 30232810

Praet J, Manyakov NV, Muchene L, Mai Z, Terzopoulos V, de Backer S, Torremans A, Guns PJ, Van De Casteele T, Bottelbergs A, Van Broeck B, Sijbers J, Smeets D, Shkedy Z, Bijnens L, Pemberton DJ, Schmidt ME, Van der Linden A, Verhoye M. 2018. Diffusion kurtosis imaging allows the early detection and longitudinal follow-up of amyloid-β-induced pathology. *Alzheimer's Research & Therapy* **10**:8. DOI: https://doi.org/10.1186/s13195-017-0329-8, PMID: 29370870

Prasloski T, Rauscher A, MacKay AL, Hodgson M, Vavasour IM, Laule C, Mädler B. 2012. Rapid whole cerebrum myelin water imaging using a 3D GRASE sequence. *NeuroImage* **63**:533–539. DOI: https://doi.org/10.1016/j.neuroimage.2012.06.064, PMID: 22776448

Pun TW, Odrobina E, Xu QG, Lam TY, Munro CA, Midha R, Stanisz GJ. 2005. Histological and magnetic resonance analysis of sciatic nerves in the tellurium model of neuropathy. *Journal of the Peripheral Nervous System : JPNS* **10**:38–46. DOI: https://doi.org/10.1111/j.1085-9489.2005.10107.x, PMID: 15703017

Raudenbush SW. 2009. Analyzing effect sizes: Random-effects models. In: Hedges L. V (Ed). *The Handbook of Research Synthesis and Meta-Analysis,*. Russell Sage Foundation. p. 295–315.

Reeves C, Tachrount M, Thomas D, Michalak Z, Liu J, Ellis M, Diehl B, Miserocchi A, McEvoy AW, Eriksson S, Yousry T, Thom M. 2016. Combined *ex vivo* 9.4 T MRI and Quantitative Histopathological Study in Normal and Pathological Neocortical Resections in Focal Epilepsy. *Brain Pathology* **26**:319–333. DOI: https://doi.org/10.1111/bpa.12298, PMID: 26268959

Rooney WD, Johnson G, Li X, Cohen ER, Kim SG, Ugurbil K, Springer CS. 2007. Magnetic field and tissue dependencies of human brain longitudinal 1h2o relaxation in vivo. *Magnetic Resonance in Medicine* **57**:308–318. DOI: https://doi.org/10.1002/mrm.21122, PMID: 17260370

Sampaio-Baptista C, Johansen-Berg H. 2017. White matter plasticity in the adult brain. *Neuron* **96**:1239–1251. DOI: https://doi.org/10.1016/j.neuron.2017.11.026, PMID: 29268094

Schmierer K, Scaravilli F, Altmann DR, Barker GJ, Miller DH. 2004. Magnetization transfer ratio and myelin in postmortem multiple sclerosis brain. *Annals of Neurology* **56**:407–415. DOI: https://doi.org/10.1002/ana.20202, PMID: 15349868

Schmierer K, Tozer DJ, Scaravilli F, Altmann DR, Barker GJ, Tofts PS, Miller DH. 2007a. Quantitative magnetization transfer imaging in postmortem multiple sclerosis brain. *Journal of Magnetic Resonance Imaging* **26**:41–51. DOI: https://doi.org/10.1002/jmri.20984, PMID: 17659567

Schmierer K, Wheeler-Kingshott CA, Boulby PA, Scaravilli F, Altmann DR, Barker GJ, Tofts PS, Miller DH. 2007b. Diffusion tensor imaging of post mortem multiple sclerosis brain. *NeuroImage* **35**:467–477. DOI: https://doi.org/10.1016/j.neuroimage.2006.12.010, PMID: 17258908

Schmierer K, Wheeler-Kingshott CA, Tozer DJ, Boulby PA, Parkes HG, Yousry TA, Scaravilli F, Barker GJ, Tofts PS, Miller DH. 2008. Quantitative magnetic resonance of postmortem multiple sclerosis brain before and after fixation. *Magnetic Resonance in Medicine* **59**:268–277. DOI: https://doi.org/10.1002/mrm.21487, PMID: 18228601

Schmierer K, Parkes HG, So PW, An SF, Brandner S, Ordidge RJ, Yousry TA, Miller DH. 2010. High field (9.4 tesla) magnetic resonance imaging of cortical grey matter lesions in multiple sclerosis. *Brain* **133**:858–867. DOI: https://doi.org/10.1093/brain/awp335, PMID: 20123726

Seehaus A, Roebroeck A, Bastiani M, Fonseca L, Bratzke H, Lori N, Vilanova A, Goebel R, Galuske R. 2015. Histological validation of high-resolution DTI in human post mortem tissue. *Frontiers in Neuroanatomy* **9**:98. DOI: https://doi.org/10.3389/fnana.2015.00098, PMID: 26257612

Sled JG. 2018. Modelling and interpretation of magnetization transfer imaging in the brain. *NeuroImage* **182**: 128–135. DOI: https://doi.org/10.1016/j.neuroimage.2017.11.065, PMID: 29208570

Soustelle L, Antal MC, Lamy J, Rousseau F, Armspach JP, Loureiro de Sousa P. 2019. Correlations of quantitative MRI metrics with myelin basic protein (MBP) staining in a murine model of demyelination. *NMR in Biomedicine* **32**:e4116. DOI: https://doi.org/10.1002/nbm.4116, PMID: 31225675

Stanisz GJ, Kecojevic A, Bronskill MJ, Henkelman RM. 1999. Characterizing white matter with magnetization transfer and T(2). *Magnetic Resonance in Medicine* **42**:1128–1136. DOI: https://doi.org/10.1002/(SICI)1522-2594(199912)42:6<1128::AID-MRM18>3.0.CO;2-9, PMID: 10571935

Stanisz GJ, Webb S, Munro CA, Pun T, Midha R. 2004. MR properties of excised neural tissue following experimentally induced inflammation. *Magnetic Resonance in Medicine* **51**:473–479. DOI: https://doi.org/10.1002/mrm.20008, PMID: 15004787

Takagi T, Nakamura M, Yamada M, Hikishima K, Momoshima S, Fujiyoshi K, Shibata S, Okano HJ, Toyama Y, Okano H. 2009. Visualization of peripheral nerve degeneration and regeneration: monitoring with diffusion tensor tractography. *NeuroImage* **44**:884–892. DOI: https://doi.org/10.1016/j.neuroimage.2008.09.022, PMID: 18948210

Tardif CL, Bedell BJ, Eskildsen SF, Collins DL, Pike GB. 2012. Quantitative magnetic resonance imaging of cortical multiple sclerosis pathology. *Multiple Sclerosis International* **2012**::1–13. DOI: https://doi.org/10.1155/2012/742018, PMID: 23213531

Thiessen JD, Zhang Y, Zhang H, Wang L, Buist R, Del Bigio MR, Kong J, Li X-M, Martin M. 2013. Quantitative MRI and ultrastructural examination of the cuprizone mouse model of demyelination. *NMR in Biomedicine* **26**: 1562–1581. DOI: https://doi.org/10.1002/nbm.2992

Tu T-W, Williams RA, Lescher JD, Jikaria N, Turtzo LC, Frank JA. 2016. Radiological-pathological correlation of diffusion tensor and magnetization transfer imaging in a closed head traumatic brain injury model. *Annals of Neurology* **79**:907–920. DOI: https://doi.org/10.1002/ana.24641

Turati L, Moscatelli M, Mastropietro A, Dowell NG, Zucca I, Erbetta A, Cordiglieri C, Brenna G, Bianchi B, Mantegazza R, Cercignani M, Baggi F, Minati L. 2015. *In vivo* quantitative magnetization transfer imaging correlates with histology during de- and remyelination in cuprizone-treated mice. *NMR in Biomedicine* **28**:327–337. DOI: https://doi.org/10.1002/nbm.3253, PMID: 25639498

Turner R. 2019. Myelin and modeling: bootstrapping cortical microcircuits. *Frontiers in Neural Circuits* **13**:34. DOI: https://doi.org/10.3389/fncir.2019.00034, PMID: 31133821

Underhill HR, Rostomily RC, Mikheev AM, Yuan C, Yarnykh VL. 2011. Fast bound pool fraction imaging of the in vivo rat brain: association with myelin content and validation in the C6 glioma model. *NeuroImage* **54**:2052–2065. DOI: https://doi.org/10.1016/j.neuroimage.2010.10.065, PMID: 21029782

van Tilborg E, Achterberg EJM, van Kammen CM, van der Toorn A, Groenendaal F, Dijkhuizen RM, Heijnen CJ, Vanderschuren L, Benders M, Nijboer CHA. 2018. Combined fetal inflammation and postnatal hypoxia causes myelin deficits and autism-like behavior in a rat model of diffuse white matter injury. *Glia* **66**:78–93. DOI: https://doi.org/10.1002/glia.23216, PMID: 28925578

Varma G, Duhamel G, de Bazelaire C, Alsop DC. 2015. Magnetization transfer from Inhomogeneously broadened lines: a potential marker for myelin. *Magnetic Resonance in Medicine* **73**:614–622. DOI: https://doi.org/10.1002/mrm.25174, PMID: 24604578

Viechtbauer W. 2010. Conducting Meta-Analyses in R with the metafor Package. *Journal of Statistical Software* **36**:i03. DOI: https://doi.org/10.18637/jss.v036.i03

Wang S, Wu EX, Cai K, Lau HF, Cheung PT, Khong PL. 2009. Mild hypoxic-ischemic injury in the neonatal rat brain: longitudinal evaluation of white matter using diffusion tensor MR imaging. *American Journal of Neuroradiology* **30**:1907–1913. DOI: https://doi.org/10.3174/ajnr.A1697, PMID: 19749219

Wang X, Cusick MF, Wang Y, Sun P, Libbey JE, Trinkaus K, Fujinami RS, Song SK. 2014. Diffusion basis spectrum imaging detects and distinguishes coexisting subclinical inflammation, demyelination and axonal injury in experimental autoimmune encephalomyelitis mice. *NMR in Biomedicine* **27**:843–852. DOI: https://doi.org/10.1002/nbm.3129, PMID: 24816651

Wang Y, Sun P, Wang Q, Trinkaus K, Schmidt RE, Naismith RT, Cross AH, Song SK. 2015. Differentiation and quantification of inflammation, demyelination and axon injury or loss in multiple sclerosis. *Brain* **138**:1223–1238. DOI: https://doi.org/10.1093/brain/awv046, PMID: 25724201

Wei H, Cao P, Bischof A, Henry RG, Larson PEZ, Liu C. 2018. MRI gradient-echo phase contrast of the brain at ultra-short TE with off-resonance saturation. *NeuroImage* **175**:1–11. DOI: https://doi.org/10.1016/j.neuroimage.2018.03.066, PMID: 29604452

Wendel KM, Lee JB, Affeldt BM, Hamer M, Harahap-Carrillo IS, Pardo AC, Obenaus A. 2018. Corpus callosum vasculature predicts white matter microstructure abnormalities after pediatric mild traumatic brain injury. *Journal of Neurotrauma* **23**:e5670. DOI: https://doi.org/10.1089/neu.2018.5670

West KL, Kelm ND, Carson RP, Gochberg DF, Ess KC, Does MD. 2018. Myelin volume fraction imaging with MRI. *NeuroImage* **182**:511–521. DOI: https://doi.org/10.1016/j.neuroimage.2016.12.067, PMID: 28025129

Wu QZ, Yang Q, Cate HS, Kemper D, Binder M, Wang HX, Fang K, Quick MJ, Marriott M, Kilpatrick TJ, Egan GF. 2008. MRI identification of the rostral-caudal pattern of pathology within the corpus callosum in the cuprizone mouse model. *Journal of Magnetic Resonance Imaging : JMRI* **27**:446–453. DOI: https://doi.org/10.1002/jmri.21111, PMID: 17968901

Yano R, Hata J, Abe Y, Seki F, Yoshida K, Komaki Y, Okano H, Tanaka KF. 2018. Quantitative temporal changes in DTI values coupled with histological properties in cuprizone-induced demyelination and remyelination. *Neurochemistry International* **119**:151–158. DOI: https://doi.org/10.1016/j.neuint.2017.10.004

Yarnykh VL. 2012. Fast macromolecular proton fraction mapping from a single off-resonance magnetization transfer measurement. *Magnetic Resonance in Medicine* **68**:166–178. DOI: https://doi.org/10.1002/mrm.23224, PMID: 22190042

Zaaraoui W, Deloire M, Merle M, Girard C, Raffard G, Biran M, Inglese M, Petry KG, Gonen O, Brochet B, Franconi J-M, Dousset V. 2008. Monitoring demyelination and remyelination by magnetization transfer imaging in the mouse brain at 9.4 T. *Magnetic Resonance Materials in Physics, Biology and Medicine* **21**:357–362. DOI: https://doi.org/10.1007/s10334-008-0141-3

Zhang J, Jones M, DeBoy CA, Reich DS, Farrell JA, Hoffman PN, Griffin JW, Sheikh KA, Miller MI, Mori S, Calabresi PA. 2009. Diffusion tensor magnetic resonance imaging of wallerian degeneration in rat spinal cord after dorsal root axotomy. *Journal of Neuroscience* **29**:3160–3171. DOI: https://doi.org/10.1523/JNEUROSCI.3941-08.2009, PMID: 19279253

Appendix 1

Search keywords

(myelin[Title/Abstract] AND ((magnetic[Title/Abstract] AND resonance[Title/Abstract]) OR mr[Title/Abstract] OR mri[Title/Abstract])) AND (histology[Title/Abstract] OR histopathology[Title/Abstract] OR microscopy[Title/Abstract] OR immunohistochemistry[Title/Abstract] OR histological[Title/Abstract] OR histologically[Title/Abstract] OR histologic[Title/Abstract] OR histopathological[Title/Abstract] OR histopathologically[Title/Abstract] OR histopathologic[Title/Abstract]).

Results obtained from the Medline database: 688 (03/06/2020).

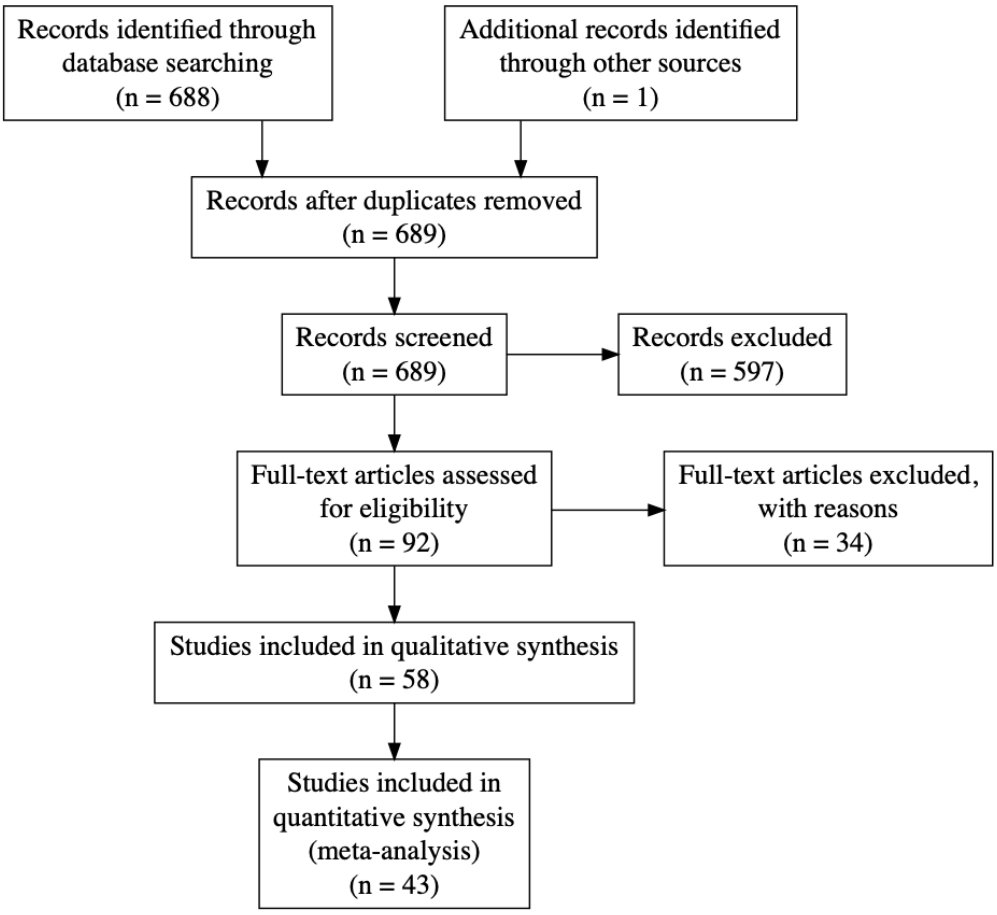

Appendix 1—figure 1. PRISMA flowchart for the meta-analysis.

Fixed- and mixed-effects models

While a traditional linear regression model estimates the error variance from residuals, in a fixed effects meta-analysis model, each paper's response and standard errors, as well as the error variance of the regression model can be directly computed from the supplied response standard deviations. Specifically, for a (non-meta) regression model we have the i-th response y_i modeled with covariate values x_i, $y_i = x_i\beta + \varepsilon_i$, where random error has unknown variance $\mathrm{Var}(\varepsilon_i) = \sigma^2$. In a fixed-effects meta-analysis, we are given y_i but also s_i, the standard error of y_i, and the regression model has the same form except the variance is known, $\mathrm{Var}(\varepsilon_i) = s_i^2$, and the weighted least squares regression can be computed, estimating beta and its standard error. A mixed-effects meta-analysis accounts for more variance than what can be ascribed to the sampling error of the reported outcome. The regression model has again the same form, except now the variance is $\mathrm{Var}(\varepsilon_i) = s_i^2 + \tau^2$, the sum of the reported squared standard error and the unknown between-study variance τ^2. Iterative methods are used to estimate τ^2 and, once estimated, a weighted least squares regression can be computed. The parameter τ^2 can be interpreted as the variance of *noise-free* (hypothetical, zero standard error)

results from the population of all possible studies. The importance of τ^2 can also be gauged by I^2, the proportion of variance due to random inter-study differences (i.e. $1 - I^2$ is the proportion attributable to random sampling error of each study) (***Higgins and Thompson, 2002***).

Abbreviations and mathematical symbols

AD – axial diffusivity
AK – axial kurtosis
AWF – axonal water fraction
FA – fraction anisotropy
ihMTR – inhomogeneous magnetization transfer ratio
k_fm – free water-macromolecular exchange rate
k_mf – macromolecular-free water exchange rate
M0m – macromolecular pool magnetization fraction
MD – mean diffusivity
MK – mean kurtosis
MPF – macromolecular pool fraction
MT – magnetization transfer
MTR – magnetization transfer ratio
MTR-UTE – magnetization transfer ratio (using ultra-short echo time)
MTV – macromolecular tissue volume
MVF-MT – myelin volume fraction (estimated from MT)
MVF-T2 – myelin volume fraction (estimated from T2)
MWF – myelin water fraction
PD – proton density
PN – peripheral nerve
PRISMA – Preferred Reporting Items for Systematic Reviews and Meta-Analyses
QSM – quantitative susceptibility mapping
R1f – free water pool longitudinal relaxation rate
R2* – apparent transverse relaxation rate
RAFF – relaxation along a fictitious field
RD – radial diffusivity
RD-DBSI – radial diffusivity (from diffusion basis spectrum imaging)
RDe – extra-cellular compartment radial diffusivity
RK – radial kurtosis
rSPF – relative semi-solid proton fraction
SC – spinal cord
T1 – longitudinal relaxation time
T1p – adiabatic longitudinal relaxation time
T1sat – longitudinal relaxation time under magnetization transfer irradiation
T2 – transverse relaxation time
T2f – free water pool transverse relaxation time
T2int – transverse relaxation intermediate component
T2m – macromolecular pool transverse relaxation rate
T2p – adiabatic transverse relaxation time

Appendix 1—table 1. Selected studies for qualitative analysis.

Study	MRI measure(s)	Histology/microscopy measure	Tissue	Condition	Focus
Schmierer et al., 2004	T1, MTR	Histology - LFB	Human	Multiple sclerosis	Brain
Odrobina et al., 2005	T1, T2, T2int, MWF, M0m, MTR	Microscopy - Myelin fraction	Animal - Rat	Demyelination - Tellurium	PN
Pun et al., 2005	T1, T2int, MWF	Microscopy - Myelin fraction	Animal - Rat	Demyelination - Tellurium	PN

Continued on next page

Appendix 1—table 1 continued

Study	MRI measure(s)	Histology/microscopy measure	Tissue	Condition	Focus
Laule et al., 2006	MWF	Histology - LFB	Human	Multiple sclerosis	Brain
Schmierer et al., 2007a	T1, MTR, MPF, T2m	Histology - LFB	Human	Multiple sclerosis	Brain
Schmierer et al., 2007b	FA, MD	Histology - LFB	Human	Multiple sclerosis	Brain
Jito et al., 2008	FA	Microscopy - Myelin sheath area	Animal - Mouse	Healthy	Brain
Kozlowski et al., 2008	MWF, FA, AD, RD, MD	Immunohistochemistry - MBP	Animal - Rat	Injury - Dorsal columnar transection	SC
Laule et al., 2008	MWF	Histology - LFB	Human	Multiple sclerosis	Brain
Schmierer et al., 2008	T1, T2, MTR, MPF, MD, FA, AD, RD	Histology - LFB	Human	Multiple sclerosis	Brain
Wu et al., 2008	T2	Histology - LFB	Animal - Mouse	Demyelination - Cuprizone	Brain
Zaaraoui et al., 2008	MTR	Immunohistochemistry - MBP	Animal - Mouse	Demyelination - Cuprizone	Brain
Takagi et al., 2009	FA, AD	EM - Myelin thickness	Animal - Rat	Degeneration - Contusive injury	PN
Wang et al., 2009	FA, RD	Histology - LFB	Animal - Rat	Ischemia - Induced hypoxia	Brain
Zhang et al., 2009	RD	Histology - LFB	Animal - Rat	Injury - Dorsal columnar transection	SC
Schmierer et al., 2010	MTR, T2	Histology - LFB	Human	Multiple sclerosis	Brain
Fatemi et al., 2011	MTR	Immunohistochemistry - MBP	Animal - Mouse	Ischemia - Induced hypoxia	Brain
Laule et al., 2011	MWF	Immunohistochemistry - MBP	Human	Multiple sclerosis	Brain
Underhill et al., 2011	MPF	Histology - LFB	Animal - Mouse	Healthy	Brain
Chandran et al., 2012	FA, RD	Immunohistochemistry - MBP	Animal - Mouse	Demyelination - Cuprizone	Brain
Tardif et al., 2012	T1, T2, MTR, PD	Immunohistochemistry - MBP	Human	Multiple sclerosis	Brain
Fjær et al., 2013	MTR	Immunohistochemistry - PLP	Animal - Mouse	Demyelination - Cuprizone	Brain
Harkins et al., 2013	MWF, MPF	Microscopy - Myelin fraction	Animal - Rat	Edema - Hexaclorophene	SC
Janve et al., 2013	MPF, R1a, k_ba, FA, RD, MD, AD	Histology - LFB	Animal - Rat	Demyelination - Lipopolysaccharide	Brain
Thiessen et al., 2013	MPF, R1f, k_fm, k_mf, T2f, T2m, MD, RD, AD, FA, T1, T2	EM - Myelin thickness	Animal - Mouse	Demyelination - Cuprizone	Brain
Kozlowski et al., 2014	MWF	Immunohistochemistry - MBP	Animal - Rat	Injury - Dorsal columnar transection	SC
Wang et al., 2014	RD, RD-DBSI	Immunohistochemistry - MBP	Animal - Mouse	Demyelination - Autoimmune encephalomyelitis	SC

Continued on next page

Appendix 1—table 1 continued

Study	MRI measure(s)	Histology/microscopy measure	Tissue	Condition	Focus
Fjær et al., 2015	MTR	Immunohistochemistry - PLP	Animal - Mouse	Demyelination - Autoimmune encephalomyelitis	Brain
Seehaus et al., 2015	FA, RD, MD	Histology - Silver	Human	Healthy	Brain
Turati et al., 2015	MPF	Immunohistochemistry - MBP	Animal - Mouse	Demyelination - Cuprizone	Brain
Wang et al., 2015	RD-DBSI	Histology - LFB	Human	Multiple sclerosis	SC
Aojula et al., 2016	FA, AD, RD, MD	Immunohistochemistry - MBP	Animal - Rat	Hydrocephalus	Brain
Hakkarainen et al., 2016	T1, T2, MTR, T1p, T2p, RAFF	Histology - Gold chloride	Animal - Rat	Healthy	Brain
Jelescu et al., 2016	RD, RK, AWF, Rde, T2, MTR	EM - Myelin fraction	Animal - Mouse	Demyelination - Cuprizone	Brain
Kelm et al., 2016	MD, RD, MK, RK, AWF	EM - Myelin fraction	Animal - Mouse	Demyelination - Knockout	Brain
Reeves et al., 2016	T1, T2	Immunohistochemistry - MBP	Human	Epilepsy	Brain
Tu et al., 2016	FA, AD, RD, MD, MTR	Immunohistochemistry - MBP	Animal - Rat	Traumatic brain injury	Brain
Chang et al., 2017	FA, AD, RD, MD	Immunohistochemistry - MBP	Animal - Mouse	Healthy	Brain
Chen et al., 2017	MWF	EM - Myelin fraction	Animal - Rat	Injury - Dorsal columnar transection	SC
Khodanovich et al., 2017	MPF	Histology - LFB	Animal - Mouse	Demyelination - Cuprizone	Brain
Lehto et al., 2017a	RAFF, MTR, T1sat, FA, MD, AD, RD	Histology - Gold chloride	Animal - Rat	Demyelination - Lipopolysaccharide	Brain
Lehto et al., 2017b	MTR	Histology - Gold chloride	Animal - Rat	Traumatic brain injury	Brain
van Tilborg et al., 2018	FA	Immunohistochemistry - MBP	Animal - Rat	White matter injury	Brain
Beckmann et al., 2018	MTR	Histology - LFB	Animal - Mouse	Demyelination - Cuprizone	Brain
Berman et al., 2018	MTV	EM - Myelin fraction	Animal - Mouse	Demyelination - Knockout	Brain
Hametner et al., 2018	R2*, T1, QSM	Histology - LFB	Human	Vascular diseases	Brain
Praet et al., 2018	MK, RK, AK, FA, MD, RD, AD	Immunohistochemistry - MBP	Animal - Mouse	Amyloidosis	Brain
Wendel et al., 2018	FA, AD, RD, MD	Immunohistochemistry - MBP	Animal - Mouse	Traumatic brain injury	Brain
West et al., 2018	MPF, MWF, MVF-T2, MVF-MT	EM - Myelin fraction	Animal - Mouse	Demyelination - Knockout	Brain
Yano et al., 2018	FA, RD, MD	Immunohistochemistry - PLP	Animal - Mouse	Demyelination - Cuprizone	Brain
Abe et al., 2019	FA, RD, AD	Microscopy - Myelin thickness	Animal - Mouse	Optogenetic stimulation	Brain
Duhamel et al., 2019	ihMTR, MTR	Microscopy - Fluorescence	Animal - Mouse	Healthy	Brain

Continued on next page

Appendix 1—table 1 continued

Study	MRI measure(s)	Histology/microscopy measure	Tissue	Condition	Focus
Khodanovich et al., 2019	MPF	Immunohistochemistry - MBP	Animal - Mouse	Demyelination - Cuprizone	Brain
Mollink et al., 2019	FA	Immunohistochemistry - MBP	Human	Amyotrophic lateral sclerosis	Brain
Peters et al., 2019	FA, MD	Histology - LFB	Human	Tuberous sclerosis complex	Brain
Pol et al., 2019	QSM, FA, MD	Histology - Solochrome	Animal - Mouse	Healthy	Brain
Soustelle et al., 2019	MPF, RD, MWF, rSPF	Immunohistochemistry - MBP	Animal - Mouse	Demyelination - Cuprizone	Brain
Guglielmetti et al., 2020	MTR, MTR-UTE	Immunohistochemistry - MBP	Animal - Mouse	Healthy	Brain